Chapter 10
The Design of Porous Organic Salts with Hierarchical Process

Norimitsu Tohnai

Abstract Porous organic materials have attracted significant attention due to their design flexibility and functional versatility. Recently, a new and widely applicable strategy for the efficient construction of versatile porous organic materials using organic salts containing triphenylmethylamine (TPMA) and sulfonic acids was reported. Combinations of TPMA and sulfonic acids with polyaromatic moieties represent a new class of porous structures consisting of diamondoid networks, termed diamondoid porous organic salts (*d*-POS) herein. In a *d*-POS, the TPMA and sulfonic acid assemble into stable tetrahedral supramolecular clusters through charge-assisted hydrogen bonding, representing the initial building blocks. These clusters subsequently accumulate via π-π interactions between polyaromatic moieties, such that the d-POS is generated. As a result of the significant steric hindrance associated with such clusters, the diamondoid network cannot build a highly interpenetrating structure, resulting in the formation of continuous open channels. It should be noted that the extent of interpenetration in the diamondoid networks can be controlled by adjusting the bulkiness of the clusters by changing the sulfonic acid. Anthracene-2-sulfonic acid (2-AS) builds a three-fold structure with one-dimensional channels, while pyrene-1-sulfonic acid produces a two-fold structure with two-dimensional channels. In addition, organic salts composed of TPMA and 2-AS also provide polymorphic structures depending on the ratio of pores to template molecules and the template species. These structures demonstrate the stability and flexibility of *d*-POS materials.

Keywords Organic salt · Charge-assisted hydrogen bond · Porous structure · Diamondoid network · Crystal engineering

N. Tohnai (✉)
Department of Applied Chemistry, Graduate School of Engineering, Osaka University, Yamadaoka 2-1, Suita, Osaka 565-0871, Japan
e-mail: tohnai@chem.eng.osaka-u.ac.jp

M. Sakamoto and H. Uekusa (eds.), *Advances in Organic Crystal Chemistry*,
https://doi.org/10.1007/978-981-15-5085-0_10

10.1 Introduction

The construction of porous structures using small organic compounds is of significant interest, and this technique has a wide range of applications related to gas and molecular storage [1] as well as the fabrication of template response materials, including chemical sensors [2]. Recently, the strategic construction of porous structures, such as metal–organic frameworks (MOFs) [3] and covalent-organic frameworks (COFs) [4], has attracted attention because such techniques provide efficient synthetic strategies and molecular compatibility. These structures are generated via the formation of either coordination or covalent bonds and thus are robust. However, organic porous structures held together by weak non-covalent bonds are also an attractive alternative, due to their processing advantages and good workability [5]. As an example, porous structures can be designed based on organic ammonium sulfonate salts [6]. Organic salt systems comprising two components allow systematic structural design simply by varying the combination of materials. In addition, ammonium sulfonate ion pairs generate strong intermolecular hydrogen bonding and electrostatic interactions. Over the past 20 years, Ward et al. have studied a variety of porous structures based on guanidine and disulfonic acids [7]. In these structures, two-dimensional hydrogen-bonded sheets containing guanidinium and sulfonate ions are connected by disulfonate pillars to produce a grid-like structure with one-dimensional open channels. Our own group has previously reported the preparation of organic structures consisting of sulfonic acids and aliphatic amines, termed porous organic salts (POSs) [8]. As an example, biphenyl-4,4′-disulfonic acid and aliphatic primary amines can be employed to build a POS with a layered network via charge-assisted hydrogen bonding [8a]. The size and shape of the void spaces in such materials can be readily adjusted simply by changing the amine. These POS systems are expected to provide tunable substances with highly versatile functions due to the variety of possible combinations of sulfonic acids and amines.

Herein, a new and efficient strategy for building porous structures with diamondoid networks is proposed, using the POS approach. The construction of such structures is attractive not only as a means of obtaining highly symmetric, well-shaped networks, but also because these materials can provide high stiffness, good stability, and large voids. Since the first report of a stable organic diamondoid network of tetrahedral tetracarboxylic acid derivatives in 1988 by Ermer, [9] several porous materials utilizing similar single tetrahedral molecules as building blocks have been prepared [10]. However, it is still difficult to achieve the desired diversity in such structures using this conventional strategy. This is because the structural design of the diamondoid network often restricts the molecular configuration to a tetrahedral shape that cannot be further modified. In addition, these diamondoid networks tend to form highly interpenetrating structures [11], in which void spaces are smaller or absent due to the use of “non-bulky” building blocks. To overcome these problems, a supramolecular-based hierarchical strategy is proposed, in which tetrahedral supramolecules formed by simple molecules are employed as

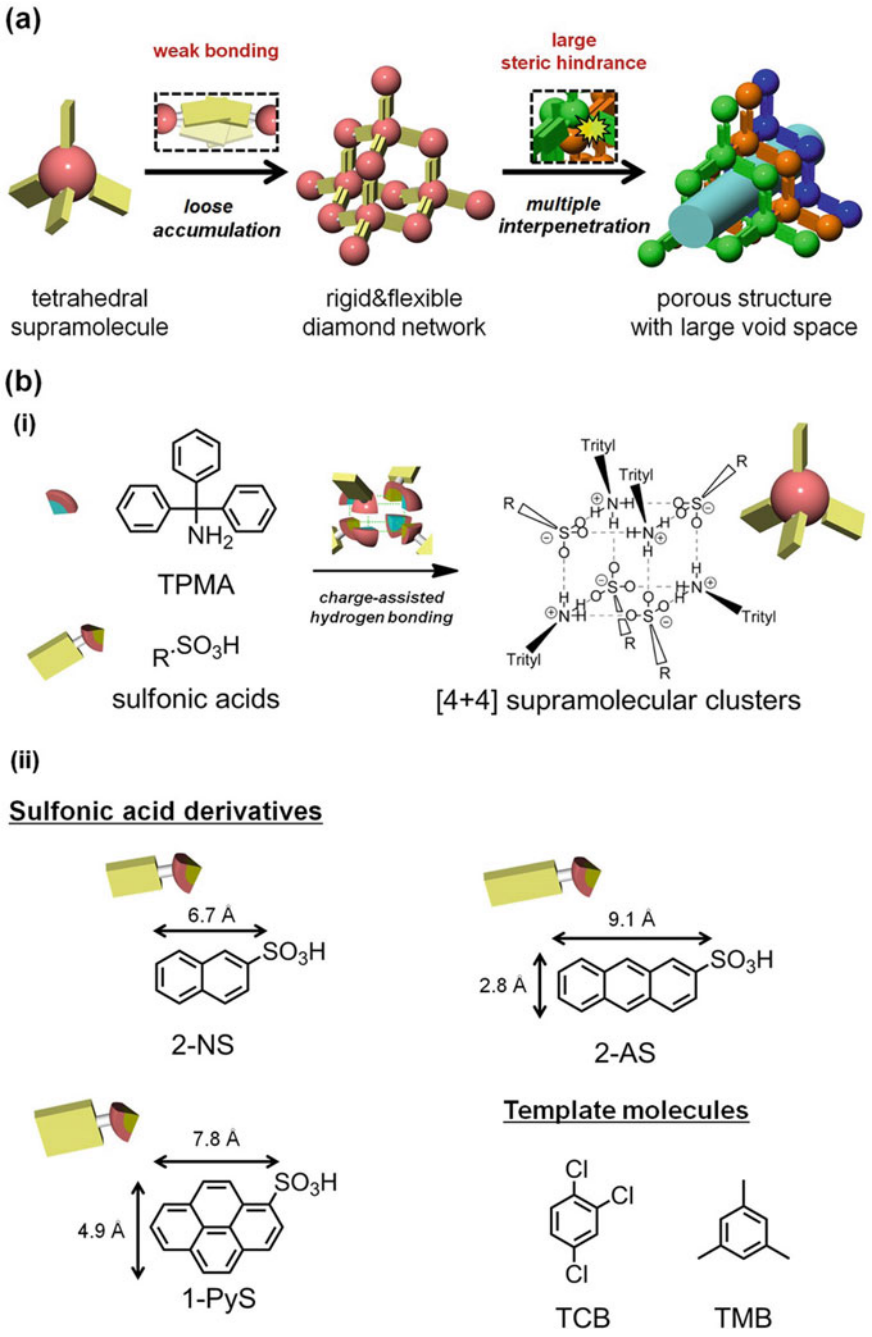

Fig. 10.1 **a** Proposed supramolecular-based hierarchical strategy. **b** [4 + 4] supramolecular cluster constructed of TPMA and sulfonic acid derivatives (i) and chemical structures of sulfonic acid derivatives and template molecules (ii). The distances are defined between a carbon or sulfur atom and any carbon atoms

building blocks for fabrication of the diamondoid network (Fig. 10.1a). Tetrahedral supramolecules are expected to act as sterically bulky nodes that prevent the diamondoid network from forming a highly interpenetrating structure. Previously, a specific type of supramolecule was also reported, termed a [4 + 4] supramolecular cluster. This compound was made of organic salts comprising triphenylmethylamine (TPMA) and monosulfonic acid derivatives (Fig. 10.1b, i). Within these clusters, the sulfonic acid derivatives are always arranged in tetrahedra as a result of cubic charge-assisted hydrogen bonding. Specific tetrahedral supramolecular clusters were designed that combined TPMA and monosulfonic acid derivatives with polycyclic aromatic moieties to produce diamondoid networks. In these substances, the long aromatic moieties protruding in the tetrahedral direction also function as a supramolecular adhesive that connects clusters via π-π interactions [12], thus generating not only rigid but also flexible (amphoteric) diamondoid networks and porous structures. These amphoteric structures are expected to provide more static and dynamic responses to external stimuli than are obtained with some flexible MOFs [2b, c, 3c]. Furthermore, the size, shape, and functionality of the clusters are dependent on the specific sulfonic acid derivative employed. In the present work, three different sulfonic acid derivatives were combined with TPMA: naphthalene-2-sulfonic acid (2-NS, 1), anthracene-2-sulfonic acid (2-AS, 2) [13], and pyrene-1-sulfonic acid (1-PyS, 3) [14] (Fig. 10.1b, ii). Organic salts containing either 2-AS or 1-PyS were used to construct diamondoid networks and interpenetrated porous structures containing aromatic molecules as templates. Interestingly, the degree of interpenetration of these diamondoid networks can be controlled by adjusting the bulkiness of the clusters, resulting in the formation of voids with various sizes and dimensions. In addition, the 2-AS diamondoid network changes structure depending on the ratio of pores to template molecules and the type of template.

10.2 Hierarchical Construction of d-POSs

The organic salts made by combining 2-AS and TPMA in the present work were recrystallized from a mixture of ethanol and nonpolar solvents such as aromatic hydrocarbons and appeared as yellow crystals. Single crystals suitable for single X-ray crystallographic analysis were obtained by recrystallization from a mixture of ethanol and 1,2,4-trichlorobenzene (TCB) [15]. This crystallographic analysis established that the crystals had a porous structure based on a diamondoid network, and so the materials produced in this work are generally referred to herein as diamondoid POSs (*d*-POSs) (specifically, *d*-POS-2a, Fig. 10.2a). Figure 10.2c illustrates the manner in which the *d*-POS-2a structure was built hierarchically, starting with 2-AS and TPMA (Fig. 10.2c). In the first step, the 2-AS and TPMA are assembled into [4 + 4] supramolecular clusters due to the effects of charge-assisted hydrogen bonding. The length of the hydrogen bond between the oxygen atom of the 2-AS and the nitrogen atom of the TPMA ranged from 2.735 to 2.863 Å (Fig. 10.3a). These hydrogen bonds produced a cubic network. However, because the anthracenyl

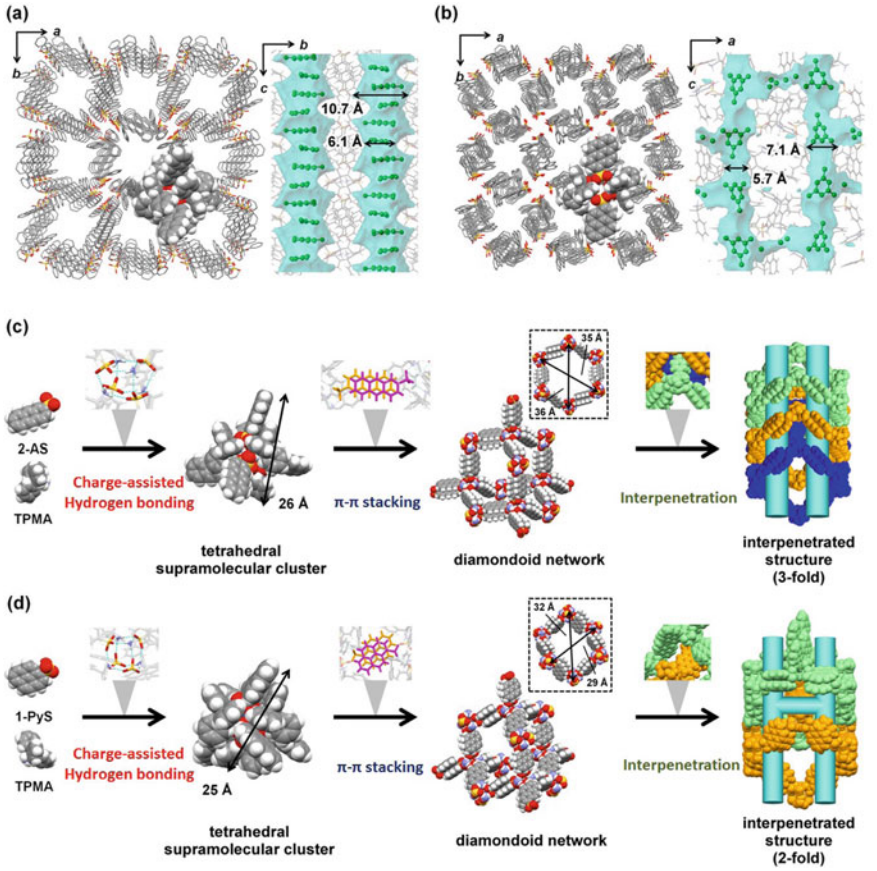

Fig. 10.2 Crystal structures of *d*-POSs. Top view and void space of d-POSs **a** composed of 2-AS and TPMA including TCB (***d*-POS-2a**) and **b** 1-PyS and TPMA including TMB (***d*-POS-3**). In the top view, template molecules are omitted for clarity. In the sky-blue-colored void space, template molecules are represented by green balls and sticks. Hydrogen atoms are omitted for clarity except in the space-filling model of a cluster. Hierarchical interpretation of **c *d*-POS-2a** and **d *d*-POS-3**. In the diamondoid networks and interpenetrated structures, triphenylmethyl groups are omitted for clarity. The independent diamondoid networks are indicated by orange, green, and blue

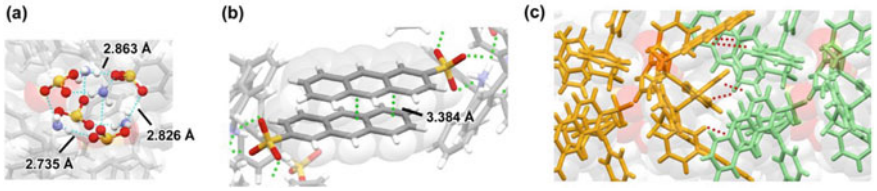

Fig. 10.3 **a** Cubic-like hydrogen bonding network in the tetrahedral supramolecular cluster. **b** π-π stacking manners between the clusters in *d*-POS-2a. **c** Close up view between the clusters in different diamondoid networks. Red lines represent CH-π intercluster contacts

group is much longer than the triphenylmethyl group, the cluster is tetrahedral and the maximum distance between the sulfur and carbon atoms is 9.1 Å (Figs. 10.1b and 10.2c). The maximum distance between the adjacent sides of the tetrahedral cluster in this structure is approximately 26 Å. Subsequently, the anthracenyl groups undergo π-π stacking and serve as linkers to arrange the clusters into a diamondoid network (Fig. 10.2c) in which the average distance between the aromatic moieties is 3.384 Å (Fig. 10.3b). This network contains very large voids associated with 35 × 36 Å hexagonal windows and three independent diamondoid networks penetrate one another to fill such voids. Nevertheless, the interpenetrating structure still possesses one-dimensional (1D) voids containing TCB molecules from the recrystallization solvent that act as template molecules (Fig. 10.2c, a, right). The bulkiness of the supramolecular clusters at the tetrahedral nodes plays an important role in creating the voids, and the diameter of the spherical core covered with triphenylmethyl groups in the clusters is approximately 16 Å. This bulkiness leads to significant steric hindrance between the nodes that prevents the formation of highly interpenetrating structures and inhibits complete filling of the voids (Fig. 10.3c). Calculations using the PLATON/VOID software package established that the void volume was 30% [16], the maximum void area was 10.7 × 10.7 Å, and the minimum was 6.1 × 6.1 Å (Fig. 10.2a, right). Each void was found to contain four TCB molecules per cluster. Interestingly, these template molecules were arranged almost parallel to one another (Fig. 10.2a, right, and Fig. 10.4), with a distance between adjacent molecules of 3.930 Å. The template molecules also adjusted the arrangement in the void space based on CH-Cl contact, while the void surfaces were covered by the aromatic rings. The effective CH-Cl contact between the template molecule and the wall contributes significantly to the specific parallel arrangement. Highly interpenetrating structures are generally considered undesirable because they tend

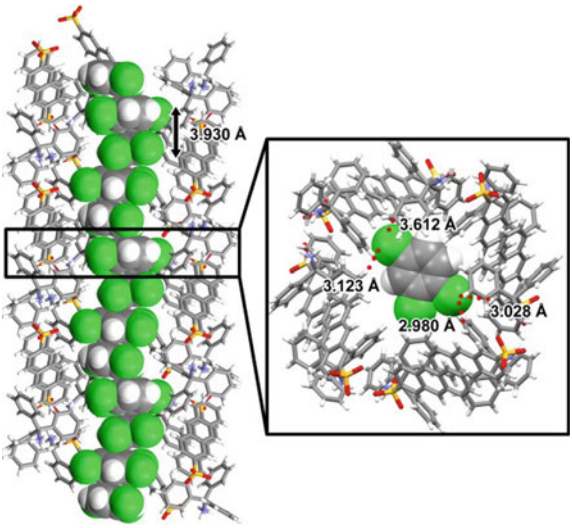

Fig. 10.4 1D array of the template molecules in the *d*-POS-2a

to reduce the void volume. However, in this material, the characteristic arrangement of template molecules is confined by the 1D voids formed by three interpenetrating diamondoid networks. This 1D molecular array could result in unique properties such as polarization performance and anisotropic charge conduction [17].

10.3 Structural Diversification of *d*-POSs with Variations in the Sulfonic Acid

Similar to the organic salt containing 2-AS, organic salts composed of 1-PyS and TPMA also formed a *d*-POS-2 type material through a similar hierarchical process (Fig. 10.2b, d). Single crystals for X-ray crystallographic analysis were obtained by recrystallization from a mixture of ethanol and 1,3,5-trimethylbenzene (TMB). According to X-ray analysis, the 1-PyS and TPMA also formed tetrahedral supramolecular clusters through charge-assisted hydrogen bonding (Fig. 10.2d), with a maximum distance between adjacent sides of the clusters of approximately 25 Å. The clusters were arranged in a diamondoid network by π-π stacking between the pyrenyl groups and the resulting diamondoid network also contained large voids with 29 × 32 Å hexagonal windows, leading to an interpenetrating structure. However, it should be noted that, unlike the three-fold interpenetration associated with the *d*-POS-2a, only two independent diamondoid networks penetrate one another in this material. Therefore, there are 2D voids in the porous structure (Fig. 10.2b, right). The 1D voids having a maximum space of 7.1 × 5.1 Å and a minimum space of 5.7 × 5.7 Å are connected by small orthogonal channels, and the calculated air gap volume is 29%. The TMB molecules from the recrystallization solvent were contained in the primary 1D voids and acted as templates. These void differences arise from variations in the shapes and sizes of the substituents in the sulfonic acid derivatives. The maximum distance between the sulfur and carbon atoms in 1-PyS is 7.8 Å, which is slightly less than that in 2-AS (Fig. 10.1b, ii). Therefore, the hexagonal windows in the *d*-POS-3 diamondoid network were smaller than the hexagonal windows in the *d*-POS-2a. In contrast, the width of 1-PyS is greater than that of 2-AS, and the maximum distances between any two carbon atoms in these compounds were 4.9 and 2.8 Å, respectively (Fig. 10.1b, ii). Therefore, 1-PyS and TPMA form more sterically bulky clusters than 2-AS and TPMA, preventing interpenetration more effectively (Fig. 10.2d). These results show that the relative ratio of the cluster core diameter to the polycyclic aromatic length has a significant effect on the avoidance of highly interpenetrating structures. When the polyaromatic group is short and wide, the relative proportion of the cluster cores increases. As a result, the resulting tetrahedral clusters exhibit increased steric hindrance and there is reduced interpenetration in the diamondoid network. In contrast, the organic salt composed of 2-NS and TPMA did not form a porous structure with a diamondoid network (Fig. 10.5). This difference can be attributed to the naphthyl groups of the 2-NS molecules (in which the maximum distance between sulfur and carbon atoms is 6.7 Å), which are too short

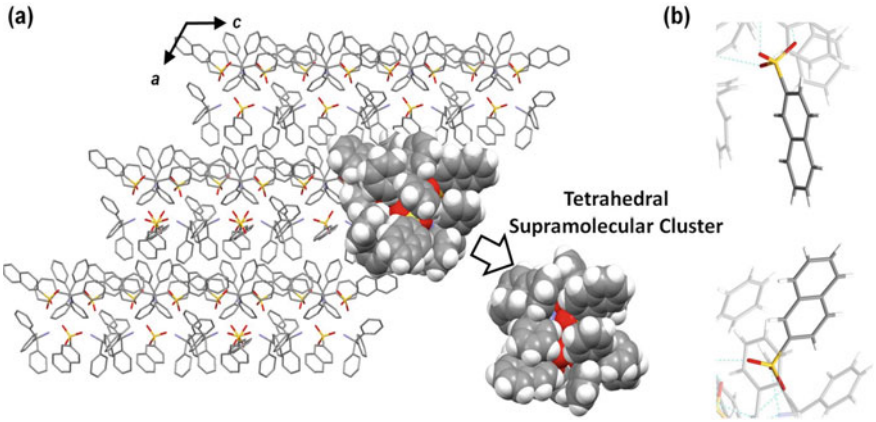

Fig. 10.5 Crystal structure composed of 2-NS and TPMA. **a** Top view of the structure. Hydrogen atoms are omitted for clarity except in the space-filling model of one supramolecular cluster. **b** Location of the naphthyl groups between neighboring clusters in the structure

to protrude from the cluster toward the tetrahedron and that do not undergo π-π interactions between themselves. Thus, the clusters form a close-packed structure without a diamondoid network. These results show that selecting the appropriate sulfonic acid derivative allows ready adjustment of the networks and the degree of interpenetration.

10.4 Structural Diversification of *d*-POSs Depending on Template Molecules

Interestingly, the diamondoid network also exhibits structural flexibility depending on the type and amount of template molecule. A typical example is the aforementioned organic salt composed of 2-AS and TPMA. The organic salt also gave two other pseudopolymorphic crystals, *d*-POS-2b and *d*-POS-2c, upon recrystallization from a mixture of ethanol and TMB. The *d*-POS-2b was obtained by slow recrystallization, while *d*-POS-2c was primarily obtained by rapid recrystallization. X-ray crystallographic analysis demonstrated that these crystals were composed of *d*-POS structures containing TMB molecules from the recrystallization solvent in 1D voids, where they served as template molecules (Fig. 10.6a, b). The *d*-POS-2b contained indented 1D voids with a maximum cross-section of 10.6 × 9.6 Å and a minimum of 4.5 × 3.0 Å (Fig. 10.6c). The void volume was determined to be 29% per unit cell using the PLATON/VOID software. In contrast, the *d*-POS-2c contained relatively straight 1D voids (Fig. 10.6d) having a maximum void size of 11.2 × 9.9 Å and a minimum size of 6.5 × 6.0 Å. Compared to the *d*-POS-2b, the voids in the *d*-POS-2c were slightly larger and had no pockets, while accounting for 36% of

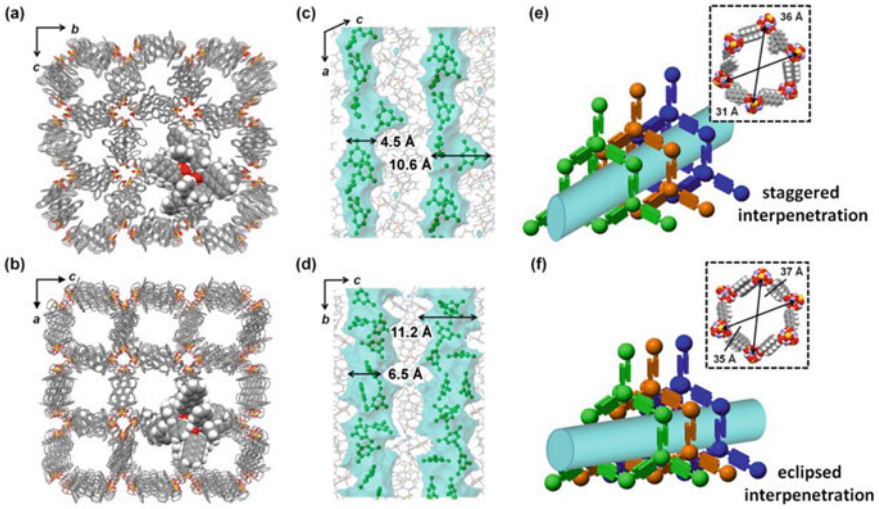

Fig. 10.6 Crystal structures of *d*-POSs composed of 2-AS and TPMA including TMB. Top view of **a *d*-POS-2b** and **b *d*-POS-2c**. In the top view, guest molecules and hydrogen atoms are omitted for clarity except for in the space-filling model of one supramolecular cluster. Visualization of the void space in **c *d*-POS-2b** and **d *d*-POS-2c**. Void spaces are indicated in sky blue, and guest molecules are represented by green sticks. Hydrogen atoms of the guests are omitted for clarity. Schematic representation of the interpenetration manners of the diamondoid networks in **e *d*-POS-2b** and **f *d*-POS-2c**

the unit cell volume. These materials were built up through the same hierarchical process as described above. That is, three independent diamondoid networks could be obtained, having the same topology and interpenetrating porous structures. These results indicate that stable diamondoid networks could be formed regardless of the template. However, the shape and size of the diamondoid networks were significantly different: the *d*-POS-2b and *d*-POS-2c diamondoid networks had 31 × 36 and 35 × 37 Å hexagonal windows (Fig. 10.6e, f, inset). This expansion and contraction of the diamondoid network is related to the template ratio. Specifically, the *d*-POS-2b incorporated three template molecules per cluster, while the *d*-POS-2c contained four. In addition, the template species also affected the structure of the diamondoid network. The *d*-POS-2c had hexagonal window that were slightly larger than the window in the material containing TCB molecules, even though both samples had the same template ratio (Fig. 10.2a, c). This difference may have occurred because TMB is slightly larger than TCB. These results demonstrate that the diamondoid networks were stable and flexible in response to changes in the template molecule. Such behavior is clearly different from that of conventional diamondoid networks based on strong interactions such as covalent bonds. The flexibility of the present diamondoid networks is derived not only from the malleability of the cluster conformations, but also from the ability of the π-π stacking orientation between the clusters to change. The interpenetration of the networks is also tunable (Fig. 10.7). These

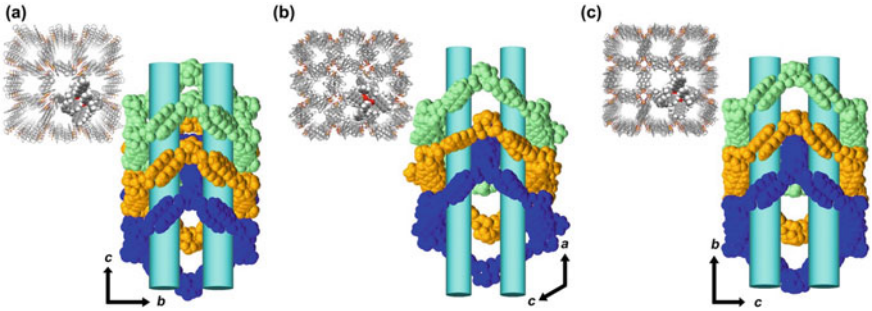

Fig. 10.7 Interpenetration manners of **a** ***d*-POS-2a**, **b** ***d*-POS-2b** and **c** ***d*-POS-2c**. The independent diamondoid networks are indicated by blue, green and orange, respectively. The blue tubes indicate the void spaces. Triphenylmethyl groups are omitted for clarity

phenomena are ascribed to the surprising stability and reproducibility of the cubic hydrogen-bonded network. As demonstrated in the previous work, this network is always formed regardless of the sulfonic acid derivative that is employed [18]. Therefore, the π-π stacking is affected by the template molecule that is used, potentially providing voids with varying shapes and sizes. The flexibility of these structures increases the degree of inclusion that is possible and renders the porous structure sensitive to external stimuli.

10.5 Structural Transformation of *d*-POSs on Template Release

To further assess the porosity of these *d*-POS materials, structural stability during template release was investigated, and thermogravimetric analysis (TGA) of *d*-POS-2a to c single crystals showed different template release profiles (Fig. 10.8). The first peak in each TGA plot is associated with the release of template molecules from the *d*-POS. The second peak, above 200 °C, occurs in conjunction with a significant mass loss, and indicates the decomposition of the host framework components. As shown in Fig. 10.8a, the *d*-POS-2a completed the release of TCB template molecules before 100 °C, after which there was no mass loss up to 200 °C. The *d*-POS-2c produced the same TMB template release profile as the *d*-POS-2a. Conversely, the *d*-POS-2b TGA data indicate a gradual mass loss that continues until decomposition of the structural components above 200 °C. These differences can likely be attributed to variations in void shapes. The voids in the *d*-POS-2b had protruding pockets that were able to incorporate template molecules, while the voids in the *d*-POS-2a and *d*-POS-2c did not have this ability. These pockets would presumably allow the structure to hold the template molecules more steadily, leading to a gradual release at higher temperatures.

As shown in Fig. 10.9, powder X-ray diffraction (PXRD) analyses confirmed the high degree of crystallinity of these crystals even after template release. PXRD data

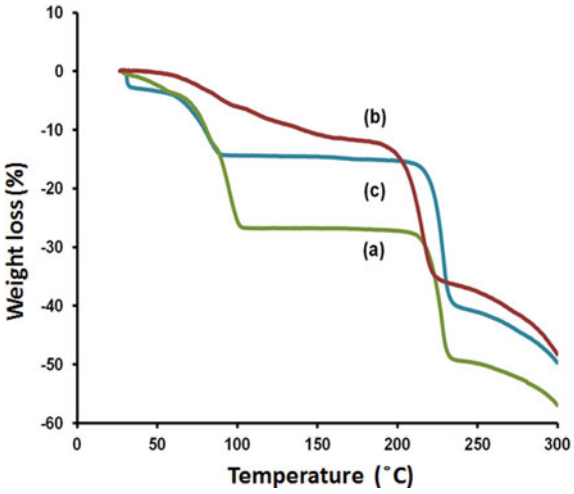

Fig. 10.8 TGA data of the d-POSs: **a *d*-POS-2a**, **b *d*-POS-2b**, and **c *d*-POS-2c**

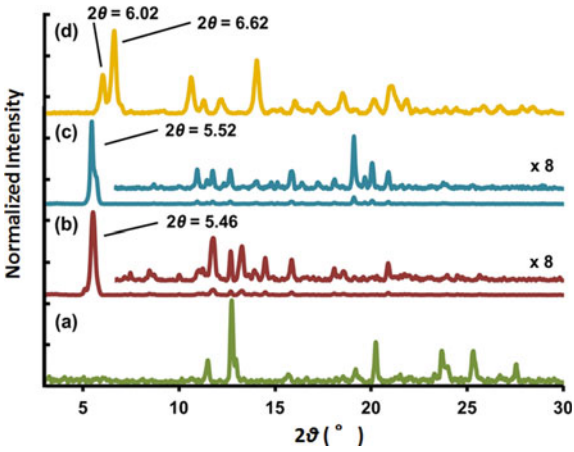

Fig. 10.9 PXRD patterns of the *d*-POSs: **a *d*-POS-2a**, **b *d*-POS-2b**, **c *d*-POS-2c** and **d *d*-POS-2b** after guest release

also showed that each *d*-POS was transformed to the same structure upon template release. Prior to release, the PXRD patterns for the *d*-POS-2b and *d*-POS-2c contain single sharp peaks at $2\theta = 5.46°$ ($d = 16.2$ Å) and 5.52° ($d = 16.0$ Å), respectively, corresponding to the distances between channels. These peaks disappear and two new peaks appear at 6.02° ($d = 14.7$ Å) and 6.62° ($d = 13.3$ Å) after the template release, indicating anisotropic shrinkage of the structure. Considering the shrinkage of the distance between channels (approximately 1.5–3.0 Å), the molecular arrangements and unit cells of the converted structures were not determined from the PXRD patterns, but it is believed that voids were present in the converted structures. These results indicate that these materials have potential applications in both molecular and gas storage.

10.6 Conclusion

In summary, a supramolecular-based hierarchical strategy was employed to build a new class of porous structures with diamondoid networks, termed diamondoid porous organic salts. Sterically hindered tetrahedral clusters prevent the excessive interpenetration of the diamondoid network and produce a porous structure. In addition, these diamondoid networks are easily adjusted by changing the sulfonic acid derivative, allowing control of the degree of interpenetration and number of voids. Moreover, the flexible accumulation of clusters provides flexibility and stability to the diamondoid network. The proposed strategy makes it possible to build organic porous structures with various functions. Tetrahedral clusters are evidently an excellent platform for arranging a wide range of organic molecules into tetrahedral shapes, even when the organic molecules themselves do not have a tetrahedral structure. This ability contributes to easy structural changes and functionalization of porous materials. As an example, the introduction of polycyclic aromatic groups into a porous structure could result in fluorescence properties depending on the template molecule employed. Furthermore, the porosity (size, shape, stability, etc.) of such materials can be controlled by selecting specific combinations of the two components. The extension of this strategy to other sulfonic acid derivatives has been actively investigated in order to construct unique functional organic porous structures.

References

1. (a) Sozzani, P., Bracco, S., Comotti, A., Ferretti, L., Simonutti, R.:Angew. Chem. Int. Ed. **44**, 1816−1820 (2005); (b) Mastalerz, M., Oppel, I.M.: Angew. Chem. Int. Ed. **51**, 5252−5255 (2012); (c) Yang, W., Greenaway, A., Lin, X., Matsuda, R., Blake, A., Wilson, C., Lewis, W., Hubberstey, P., Kitagawa, S., Champness, N., Schroder, M.: J. Am. Chem. Soc. **132**, 14457−14469 (2010); (d) Sudik, A.C., Millward, A.R., Ockwig, N.W., Coté, A.P., Kim, J., Yaghi, O.M.: J. Am. Chem. Soc. **127**, 7110−7118 (2005); (e) Furukawa, H., Yaghi, O.M.: J. Am. Chem. Soc. **131**, 8875−8883 (2009); (f) Tsue, H., Ishibashi, K., Tokita, S., Takahashi, H., Matsui, K., Tamura, R.: Chem. Eur. J. **14**, 6125−6134 (2008)
2. (a) Lu, Z.Z., Zhang, R., Li, Y.Z., Guo, Z.J., Zheng, H. G.: J. Am.Chem. Soc. **133**, 4172−4174 (2011); (b) Takashima, Y., Martinez, V.M., Furukawa, S., Kondo, M., Shimomura, S., Uehara, H., Nakahama, M., Sugimoto, K., Kitagawa, S.: Nat. Commun., 2−8 (2011); (c) Yanai, N., Kitayama, K., Hijikata, Y., Sato, H., Matsuda, R., Kubota, Y., Takata, M., Mizuno, M., Uemura, T., Kitagawa, S.: Nat. Mater. **10**, 787−793 (2011)ss
3. (a) Yaghi, O.M., O'Keeffe, M., Ockwing, N.W., Chae, H.K., Eddaoudi, M., Kim, J.: Nature **423**, 705−714 (2003); (b) Horike, S., Shimomura, S., Kitagawa, S.: Nat. Chem. 1, 695−704 (2009); (c) Farha, O.K., Hupp, J.T.: Acc. Chem. Res. **43**, 1166−1175 (2010)
4. (a) Coté, A.P., Benin, A.I., Ockwig, N.W., Matzger, A.J., O'Keeffe, M., Yaghi, O.M.: Science **310**, 1166−1170 (2005); (b) El-Kaderi, H.M., Hunt, J.R., Mendoza-Cortés, J.L., Côté, A.P., Taylor, R.E., O'Keeffe, M., Yaghi, O.M.: Science **316**, 268−272 (2007)
5. (a) Holst, J.R., Trewin, A., Cooper, A.I.: Nat. Chem. **2**, 915−920 (2010); (b) Tian, J., Thallapally, P.K., McGrail, B.P.: Cryst. Eng. Commun. **14**, 1909−1919 (2012)
6. (a) Su, X., Guo, D.S., Liu, Y.: Cryst. Eng. Commun. **12**, 947−952 (2010); (b) Leverd, P.C., Berthault, P., Lance, M., Nierlich, M.: Eur. J. Org. Chem., 133−139 (2000)

7. (a) Russell, V.A., Evans, C.C., Li, W.J., Ward, M.D.: Science **276**, 575−579 (1997); (b) Holman, K.T., Pivovar, A.M., Ward, M.D.: Science, **294**, 1907−1911 (2001); (c) Holman, K.T., Pivovar, A.M., Swift, J.A., Ward, M.D.: Acc. Chem. Res. **34**, 107−118 (2001)
8. (a) Mizobe, Y., Miyata, M., Hisaki, I., Tohnai, N.: Chem. Lett. **36**, 280−281 (2007); (b) Mizobe, Y., Miyata, M., Hisaki, I., Hasegawa, Y., Tohnai, N.: Org. Lett. **8**, 4295−4298 (2006); (c) Mizobe, Y., Hinoue, T., Miyata, M., Hisaki, I., Hasegawa, Y., Tohnai, N.: Bull. Chem. Soc. Jpn. **80**, 1162−1172 (2007)
9. (a) Ermer, O.: J. Am.Chem. Soc. **110**, 3747–3754 (1988); (b) Ermer, O., Eling, A.: Angew. Chem. Int. Ed. Eng. **27**, 829–833 (1988)
10. (a) Brunet, P., Simard, M., Wuest, J.D.: J. Am.Chem. Soc. **113**, 4696–4698 (1991); (b) Jones, K.M.E., Mahmoudkhani, A.H., Chandler, B.D., Shimizu, G.K.H.: Cryst. Eng. Commun. **8**, 303–305 (2006); (c) Uribe-Romo, F.J., Hunt, J.R., Furukawa, H., Klöck, C., O'Keeffe, M., Yaghi, O.M.: J. Am. Chem. Soc. **131**, 4570–4571 (2009)
11. (a) Reddy, D.S., Dewa, T., Endo, K., Aoyama, Y.: Angew. Chem. Int. Ed. **39**, 4266–4268 (2000); (b) Metrangolo, P., Meyer, F., Pilati, T., Proserpio, D.M., Resnati, G.: Chem. Eur. J. **13**, 5765–5772 (2007)
12. Desiraju, G.R.: Angew. Chem. Int. Ed. Engl. **34**, 2311–2327 (1995)
13. Acquavella, M.F., Evans, M.E., Farraher, S.W., Nèvoret, C.J., Abelt, C.J.: J. Org. Chem. **59**, 2894−2897 (1994)
14. Menger, F.M., Whitesell, L.G.: J. Org. Chem. **52**, 3793–3798 (1987)
15. CCDC 880742 (***d*-POS-1a**), 880741 (***d*-POS-2**), 881390 (***d*-POS-1b**), 881391 (***d*-POS-1c**) contain the supplementary crystallographic data. These data can be obtained free of charge from The Cambridge Crystallographic Data Centre via www.ccdc.cam.ac.uk/data_request/cif
16. Spek, A.L.: Acta Crystallogr. Sect. D **65**, 148–155 (2009)
17. Hertzach, T., Budde, F., Weber, E., Hulliger, J.: Angew. Chem. Int. Ed. **41**, 2281–2284 (2002)
18. Tohnai, N., Mizobe, Y., Doi, M., Sukata, S., Hinoue, T., Yuge, T., Hisaki, I., Matsukawa, Y., Miyata, M.: Angew. Chem. Int. Ed. **46**, 2220–2223 (2007)